

Dipole excitations in  $^{108}\text{Cd}$ A. Gade,<sup>1,\*</sup> D. Belic,<sup>2</sup> P. von Brentano,<sup>1</sup> C. Fransen,<sup>1</sup> H. von Garrel,<sup>2</sup> J. Jolie,<sup>1</sup> U. Kneissl,<sup>2</sup> C. Kohstall,<sup>2</sup> A. Linnemann,<sup>1</sup> H. H. Pitz,<sup>2</sup> M. Scheck,<sup>2</sup> F. Stedile,<sup>2</sup> and V. Werner<sup>1</sup><sup>1</sup>Institut für Kernphysik der Universität zu Köln, D-50937 Köln, Germany<sup>2</sup>Institut für Strahlenphysik der Universität Stuttgart, D-70569 Stuttgart, Germany

(Received 24 September 2002; published 12 March 2003)

A high-resolution nuclear resonance fluorescence experiment with bremsstrahlung of continuous energy has been performed on  $^{108}\text{Cd}$ , the rarest of the stable Cd isotopes. Accurate lifetimes of dipole excitations in the energy range of 2.6–3.9 MeV have been deduced. A magnetic dipole excitation at 3454 keV shows a decay pattern meeting the expectations for the  $1_{ms}^+$  state in a nucleus located on the transitional path between vibrational U(5) and  $\gamma$ -soft O(6) dynamical symmetry in the framework of the interacting boson model 2. We extended the systematics of quadrupole-octupole coupled electric dipole excitations  $1^-$  in the chain of even-mass Cd isotopes at its neutron deficient end.

DOI: 10.1103/PhysRevC.67.034304

PACS number(s): 21.10.Re, 23.20.Lv, 27.60.+j

## I. INTRODUCTION

Low-lying dipole excitations in even-even nuclei have been extensively studied during the past decades. In deformed nuclei, the existence of collective  $1^+$  magnetic dipole excitations has been predicted within the geometrical two-rotor model [1] as well as in the algebraic proton-neutron interacting boson model (IBM-2) [2]. The first observation of the so-called “scissors mode” in 1984 [3] prompted numerous successful electron and photon scattering experiments covering a wide range of mass [4–8]. The  $M1$  excitation strength is usually distributed among several  $1^+$  states forming the fragments of the scissors mode. Less is known about the scissors-mode analog in purely vibrational nuclei. Lacking deformation prevents the ground state decay of this excitation and makes the state inaccessible to the method of resonant photon scattering. The heavier even-mass Cd isotopes are generally assessed as good examples for near spherical vibrators close to the dynamical U(5) symmetry [9]. In a prior paper [10], we pointed out that in the terminology of the IBM-2,  $^{108}\text{Cd}$  is located on a transitional path between vibrational U(5) and  $\gamma$ -soft O(6) structure; and the question arises whether the deformation is already enhanced, so that the  $1_{ms}^+$  state can be observed in this nucleus with the method of resonant photon scattering.

Low-lying electric dipole excitations have been known in near spherical nuclei for a long time (see Ref. [11], and references within). The lowest-lying  $1^-$  state is interpreted as the dipole member of the quadrupole-octupole coupled  $(2_1^+ \otimes 3_1^-)^{(J^-)}$ ,  $J=1,2,3,4,5$  multiplet of negative parity. In a simple harmonic coupling scheme, this quintuplet is expected at the sum energy of the constituents:  $E(J^-) = E(2_1^+) + E(3_1^-)$ . The  $1^-$  state of this multiplet is well investigated in the heavier Cd isotopes  $^{110-116}\text{Cd}$  [11,12]. One aim of our experiment is the determination of the absolute  $B(E1; 1^- \rightarrow 0_1^+)$  transition strength in  $^{108}\text{Cd}$  to extend the

existing systematics at the neutron deficient end of the isotopic chain. In a prior paper [13], we assigned the complete quadrupole-octupole coupled multiplet of negative parity in  $^{108}\text{Cd}$  based on excitation energy and decay branching ratios, but lifetime information was unavailable. The expected strong  $E1$  transition to the ground state makes the nuclear resonance fluorescence (NRF) technique applicable. Nevertheless, from a technical point of view, scattering experiments on  $^{108}\text{Cd}$  represent a challenging task due to the low natural abundance of 0.89% only, which results in the limited availability of highly enriched target material.

## II. EXPERIMENT

The method of resonant photon scattering is known as well suited to populate states with  $J=1$  which are connected to the ground state by sufficiently large transition matrix elements [6]. In this report, this experimental probe is spin selective as well as strength selective, and the method of choice for the investigation of collective  $1^-$  and  $1^+$  excitations.

A photon scattering experiment on  $^{108}\text{Cd}$  was performed at the bremsstrahlung facility of the Dynamitron accelerator in Stuttgart [6]. The target consisted of 1.006 g metallic Cd with an enrichment of 63.9% in  $^{108}\text{Cd}$ . 0.753 g  $^{27}\text{Al}$  were added for photon flux calibration purposes. The experiment took about 100 hours with an endpoint energy of the bremsstrahlung spectrum of 4.1 MeV. Figures 1 and 2 show parts of the photon scattering spectrum of  $^{108}\text{Cd}$  observed with a Compton-shielded HPGe detector positioned at a scattering angle of  $127^\circ$ . Transitions from  $^{108}\text{Cd}$  are labeled with their energy. Sharp peak structures appear on the smooth background, resulting from the decays of the resonantly excited states of  $^{108}\text{Cd}$ . For some states, it was possible to observe the decay to the ground state as well as the transitions to the  $2_1^+$  state. The measured decay intensities yield the ratio  $\Gamma_1/\Gamma_0$  of the partial width for the decays to the  $2_1^+$  and the ground state, respectively. The observation of decays to higher-lying states than the  $2_1^+$  is usually prevented by the rapidly increasing nonresonant background towards lower energies. The other peaks could be assigned to  $^{27}\text{Al}$ , back-

\*Present address: NSCL, Michigan State University, East Lansing, MI 48824.

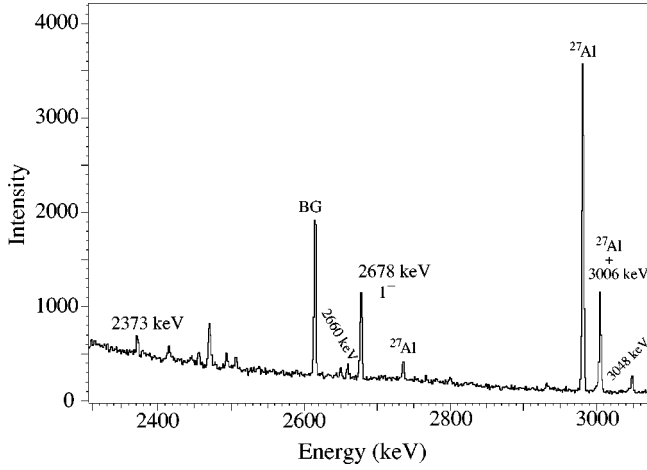


FIG. 1. Low-energy part of the NRF spectrum. Three dipole excitations (2678, 3006, and 3048 keV) of  $^{108}\text{Cd}$  as well as two transitions (2373, 2660 keV) from inelastic scattering to the  $2_1^+$  state are labeled. The 3006 keV peak forms a doublet with a peak from the  $^{27}\text{Al}$  calibration. Other peaks result from background (BG) or known even-mass  $^{110-114}\text{Cd}$  target contaminations.

ground, single escape, and contaminations from well-known (mainly even-mass) Cd isotopes in the moderately enriched target material.

The experimental setup provided the possibility to determine spin values with the method of angular correlations. Three HPGe detectors (relative efficiency 100%) were positioned at  $90^\circ$ ,  $127^\circ$  (BGO shielded), and  $150^\circ$  relative to the beam axis. The intensity ratio  $W(90^\circ)/W(127^\circ)$  offers an excellent tool to distinguish between spins  $J=2$  and  $J=1$  (Fig. 3).

Absolute, energy-integrated, elastic scattering cross sections  $I_{s,0}$  of resonantly excited states in  $^{108}\text{Cd}$  were obtained relative to the well-known cross sections of several states in the NRF calibration standard  $^{27}\text{Al}$  [14]. From these cross sections and the decay branching ratios  $\Gamma_f/\Gamma_0$  to all final

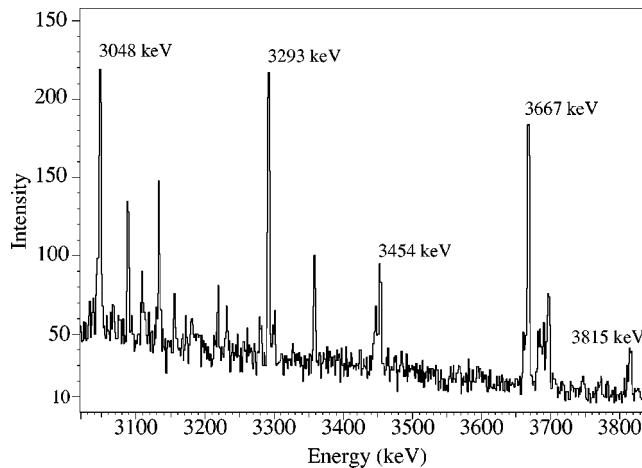


FIG. 2. High-energy part of the photon scattering spectrum. Peaks from  $^{108}\text{Cd}$  are labeled. The other peaks are known and stem from contaminations of the moderately enriched target, from  $^{27}\text{Al}$ , background or single escapes.

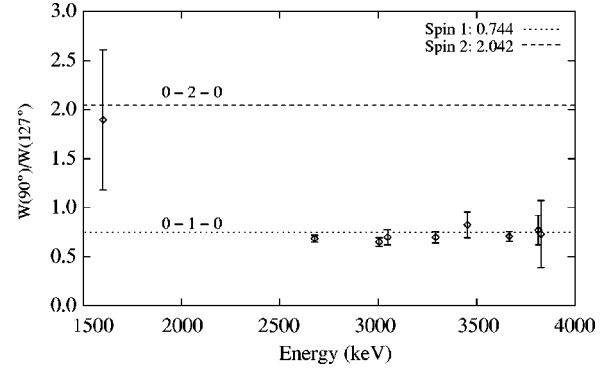


FIG. 3. Angular correlations in NRF. Compared are the intensity ratios  $W(90^\circ)/W(127^\circ)$  for the  $J^\pi \rightarrow 0_1^+$  transitions. Dipole and quadrupole transitions can be distinguished. The data point at 1602 keV stems from the ground state decay of the  $2_2^+$ .

states  $f$ , the partial decay width  $\Gamma_0$  of the level for the transition back to the ground state can be deduced:

$$\Gamma_0 = \frac{2J_0 + 1}{2J + 1} \frac{1}{(\pi \hbar c)^2} \left( 1 + \sum_{f>0} \frac{\Gamma_f}{\Gamma_0} \right) E_R^2 I_{s,0}. \quad (1)$$

The total decay width is then given by

$$\Gamma = \Gamma_0 \left( 1 + \sum_{f>0} \frac{\Gamma_f}{\Gamma_0} \right), \quad (2)$$

and provides the level lifetime model independently

$$\tau = \frac{\hbar}{\Gamma}. \quad (3)$$

In NRF experiments employing bremsstrahlung  $\gamma$  transitions with low energy tend to disappear in the high nonresonant photon scattering background. Most likely, the transition to the  $2_1^+$  state can be observed, in some cases, also the decay to the  $2_2^+$  excitation is accessible, depending on the transition energy and the branching. The accessible branching  $[1 + (\Gamma_1/\Gamma_0)] < [1 + \sum_{f>0} \Gamma_f/\Gamma_0]$  may lead to an overestimation of the lifetime and hence to the determination of an upper limit only. In the case of  $^{108}\text{Cd}$ , the decay patterns of most of the dipole excitations were observed in our  $\gamma$ - $\gamma$  coincidence studies following the  $\beta^+$  decay of the excited  $2^+$  isomer of  $^{108}\text{In}$  [15]. Therefore, extensive information on the decay properties including accurate intensity ratios and multipole mixing ratios already exists. All this information is usually inaccessible in NRF experiments with bremsstrahlung. So we were able to derive the level lifetimes  $\tau$  by combining results of the NRF measurement with data from the  $\gamma$ - $\gamma$  coincidence studies mentioned above.

We observed eight dipole excitations between 2.6 and 3.9 MeV in the present photon scattering experiment. Aside from the 3667 keV excitation, all states were also observed in Ref. [15]. The measured integrated elastic scattering cross sections  $I_{s,0}$  and lifetimes  $\tau$  are given in Tables I and II, together with branching ratios, multipole mixing ratios [15], and the deduced absolute transition strengths. Figure 4 displays the

TABLE I. Decay properties of  $1^+$  states in  $^{108}\text{Cd}$ . We list the newly established lifetimes  $\tau$ , transition energies  $E_\gamma$ , multipole mixing ratios  $\delta$  [15], branching ratios  $R$  [15], and deduced  $B(M1)$  as well as  $B(E2)$  decay strengths. The error of the branching is 20% unless particular values are given. Multipolarities marked with an asterisk are only assumed to be of pure  $E2$  character, the determination of the corresponding  $E2/M1$  mixing ratio failed.

$E_i$ (keV)	$I_{s,0}$ (eV b)	$\tau$ (fs)	$J^\pi$ ( $\hbar$ )	$E_\gamma$ (keV)	$\delta$	$J_f^\pi$ ( $\hbar$ )	$R$ (%)	$B(M1)\downarrow$ ( $\mu_N^2$ )	$B(E2)\downarrow$ ( $e^2 \text{fm}^4$ )
3048.5	8.4(5)	30(2)	$1^+$	1446.6	0.169(34)	$2_2^+$	19(3)	0.06(1)	13(2)
				2415.6	0.319(15)	$2_1^+$	62(5)	0.042(4)	11(1)
				3048.5	$M1$	$0_1^+$	100(8)	0.037(4)	
3454.1	6.5(5)	33(3)	$1^+$	1079.5	$M1$	$0_4^+$	7(5)	0.06(4)	
				1291.3	$E2^*$	$2_3^+$	7		282(48)
				1540.7	$M1$	$0_3^+$	3.3	0.009(2)	
				1733.6	$M1$	$0_2^+$	4.4	0.008(2)	
				1852.3	0.005(20)	$2_2^+$	30(9)	0.05(1)	0.005(2)
				2821.1	$\geq 11.7$	$2_1^+$	8		7(2)
3814.6	10.7(9)	21(2)	$1^+$	3454.1	$M1$	$0_1^+$	100(12)	0.024(4)	
				1194.6	$E2^*$	$2_6^+$	0.7		75(7)
				1651.7	$E2^*$	$2_3^+$	1.6		34(3)
				1901.1	$M1$	$0_3^+$	4.4	0.012(1)	
				2093.9	$M1$	$0_2^+$	2.8	0.0055(5)	
				3181.8	0.107(17)	$2_1^+$	40	0.022(2)	0.36(3)
3827.9	2.8(5)	$37_{-7}^{+9}$	$1^+$	3814.6	$M1$	$0_1^+$	100	0.033(3)	
				1207.8	$E2^*$	$2_6^+$	1		39(21)
				1453.2	$M1$	$0_4^+$	1	0.011(4)	
				1461.9	$E2^*$	$2_4^+$	4		60(20)
				1665.1	$E2^*$	$2_3^+$	4		31(11)
				1914.5	$M1$	$0_3^+$	18	0.018(5)	
				2107.3	$M1$	$0_2^+$	1.5	0.0011(4)	
				2226.2	-0.060(17)	$2_2^+$	72	0.04(1)	0.5(1)
3194.9	$E2^*$	$2_1^+$	7		2.1(8)				
3827.9	$M1$	$0_1^+$	100	0.012(3)					

ground state decay strengths of all dipole excitations observed in NRF.  $E1$  and  $M1$  scales are given. Due to low coincidence statistics caused by the lack of sufficiently enriched target material, it was not possible to use the Stuttgart Compton polarimeter for determination of parities.

### III. MAGNETIC DIPOLE EXCITATIONS

In Table I, the important decay properties of the dipole excitations with assured positive parity are listed. Decays to

higher-lying excited states as well as all intensity and multipole mixing ratios were observed in  $\gamma$ - $\gamma$  spectroscopy following the  $\beta^+$  decay of a  $2^+$  isomer of  $^{108}\text{In}$  [10,13,15]. We stress that for the states at 3454, 3815, and 3828 keV, more (weak) transitions could be established [15], but these decays are not of interest for the present discussion due to lack of knowledge about the spins of the final states and the multipolarities involved. The complete decay pattern of these excitations is presented in Ref. [15], but the very important

TABLE II. Decay properties of the  $(2_1^+ \otimes 3^-)^{(1^-)}$  excitation and of states with unknown parity. Due to weak or vanishing population of these states in the  $\beta^+$  decay of the  $2^+$  isomer of  $^{108}\text{In}$  negative parity is more likely but a final proof failed. For the decays to the ground state, we give the  $B(\sigma\pi)$  strengths for pure  $E1$  and  $M1$  radiation, for the transitions to the  $2_1^+$  state also pure  $E2$  character is considered.

$E_i$ (keV)	$I_{s,0}$ (eV b)	$\tau$ (fs)	$J^\pi$ ( $\hbar$ )	$E_\gamma$ (keV)	$\delta$	$J_f^\pi$ ( $\hbar$ )	$B(E1)\downarrow$ ( $10^{-3}e^2 \text{fm}^2$ )	$B(M1)\downarrow$ ( $\mu_N^2$ )	$B(E2)\downarrow$ ( $e^2 \text{fm}^4$ )
2678.0	26.9(9)	39.3(14)	$1^-$	2678.0	$E1$	$0_1^+$	0.83(3)		
3005.6	31.1(12)	18.7(8)	1	3005.6		$0_1^+$	0.85(9)	0.077(8)	
				2372.6	0.060(48) <sup>a</sup>	$2_1^+$	0.78(5)	0.070(4)	0.65(5)
3292.8	13.8(6)	24(1)	1	3292.8		$0_1^+$	0.51(2)	0.046(2)	
				2659.8		$2_1^+$	0.43(5)	0.039(5)	80(12)
3667.0	30.3(13)	18.6(8)	1	3667.0		$0_1^+$	0.69(3)	0.06(2)	

<sup>a</sup>From Ref. [15].

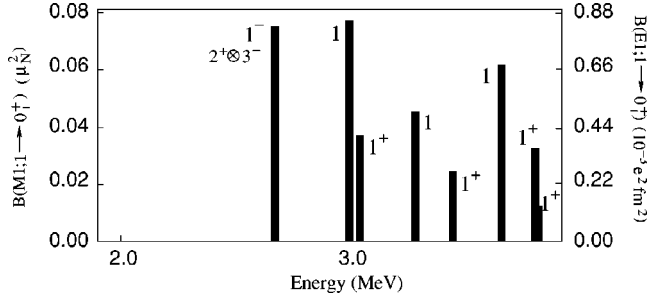


FIG. 4. Absolute deexcitation strengths in  $^{108}\text{Cd}$ .  $B(M1)\downarrow$  as well as  $B(E1)\downarrow$  scales are given.

lifetime information was absent and is provided by the present NRF experiment for the first time.

The mixed-symmetry  $1_{ms}^+$  state can be understood as the dipole member of the  $(2_1^+ \otimes 2_{ms}^+)^{(J^+)}$  coupled multiplet. The  $2_1^+$  and  $2_{ms}^+$  states are manifestations of the fundamental quadrupole degrees of freedom. The first collective  $2^+$  state in even-even nuclei represents the isoscalar quadrupole excitation in the valence shell with the isovector  $2_{ms}^+$  state as the proton-neutron antisymmetric counterpart. The  $2_{ms}^+$  state has been identified in nuclei of different mass regions:  $A \approx 100$  [16–19],  $A \approx 130$  [20–24], and  $A \approx 140$  [25–27] and recently also in  $^{108}\text{Cd}$  [10,15]. In a harmonic coupling scheme, the  $1_{ms}^+$  state is expected at the sum energy of the constituents  $E(1_{ms}^+) = E(2_1^+) + E(2_{ms}^+)$ . In measurements on  $^{94}\text{Mo}$ , the underlying two-phonon character of the  $1_{ms}^+$  state was proved [17]. The  $2_{ms}^+$  excitation in  $^{108}\text{Cd}$  was found to be fragmented into three  $2^+$  states at 2163, 2366, and 2620 keV with the latter state as the strongest fragment [15]. The high degree of fragmentation for the  $2_{ms}^+$  state already implies a comparable situation for the coupled  $1_{ms}^+$  excitation and complicates its identification in  $^{108}\text{Cd}$ .

As pointed out in Ref. [15], the state at 3454 keV shows a decay pattern meeting the expectations for a  $1_{ms}^+$  state in a transitional nucleus between the vibrational  $U(5)$  and the  $\gamma$ -soft  $O(6)$  dynamical symmetry. The signatures are a weakly collective  $E2$  decay to the  $2_1^+$  state, a strong  $M1$  transition to the  $2_2^+$  state, a collective  $E2$  transition to the mixed-symmetry  $2_{ms}^+$  state and, depending on the underlying dynamical symmetry, an  $M1$  transition to the ground state (Fig. 5). This ground state decay is a tool to estimate the position of  $^{108}\text{Cd}$  on the mentioned transitional path between spherical and  $\gamma$ -soft deformation. In the IBM-2, the ground state in the  $U(5)$  limit is the  $d$ -boson vacuum, while the  $O(6)$  ground state has a nonvanishing expectation value  $\langle n_d \rangle$  for the number of  $d$  bosons [28]. The usual one-body  $T(M1)$  operator cannot mediate a transition from the  $1_{ms}^+$  state to the  $d$ -boson vacuum, therefore  $B(M1; 1_{ms}^+ \rightarrow 0_1^+) = 0$  holds in the pure  $U(5)$  limit. Increasing deviation from the pure  $U(5)$  limit towards  $O(6)$  symmetry leads to a sizable  $B(M1; 1_{ms}^+ \rightarrow 0_1^+)$  transition strength. The most basic Hamiltonian between these symmetry limits is given by

$$H = \epsilon n_d - \kappa (Q_\pi^{\chi=0} + Q_\nu^{\chi=0})^2 + \lambda M_{\pi\nu}, \quad (4)$$

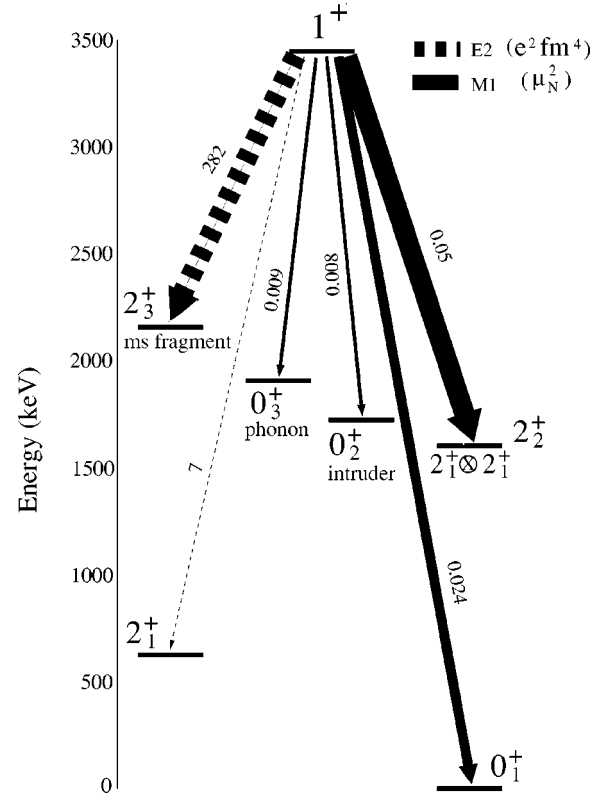


FIG. 5. Decay properties of the  $1_{ms}^+$  candidate at 3454 keV [15] (see Table I). This state shows the expected  $M1$  and  $E2$  decay pattern characteristic for a “scissors-mode-like” state between the dynamical  $O(6)$  and  $U(5)$  symmetry in the framework of the IBM-2. The decay to the ground state of the intruder band suggests non-negligible quasiparticle contributions in the wave function.

with the  $d$ -boson number operator  $n_d$  and the  $F$ -spin symmetric quadrupole-quadrupole interaction. The Majorana interaction  $M_{\pi\nu}$  [29] can be neglected for the present discussion, because it only affects the position of the mixed-symmetry states and leaves the wave functions unchanged. Pure  $U(5)$  symmetry is reached with  $\kappa=0$ , while  $\epsilon=0$  is required for a description of the pure  $O(6)$  limit. In the vicinity of pure symmetry limits, the  $B(M1)$  strengths are given analytically as a function of the proton and neutron boson numbers  $N_\pi$  and  $N_\nu$  [30]. Using the simple Hamiltonian (4) the  $B(M1)$  values scale with  $\epsilon/\kappa$  along the transitional path between the dynamical symmetries  $U(5)$  and  $O(6)$ . In Fig. 6 we show the evolution of absolute  $M1$  transition strength as a function of  $\epsilon/\kappa$ .  $0 \leq \epsilon/\kappa \leq \infty$  covers the transition between the symmetry limits. The decay strength to the ground state clearly undergoes a rapid change, while the  $M1$  strength to the  $2_2^+$  remains rather constant. These calculations for a nucleus with  $N_\pi=1$  and  $N_\nu=5$  were performed with the IBM-2 code NPBOS [31].

The experimental ratio

$$\frac{B(M1; 1_{3454}^+ \rightarrow 2_2^+)}{B(M1; 1_{3454}^+ \rightarrow 0_1^+)} = 2.1(5) \quad (5)$$

can be reproduced within the IBM-2 using  $\epsilon/\kappa=2$  in Hamiltonian (4). Now it will be interesting to investigate if this

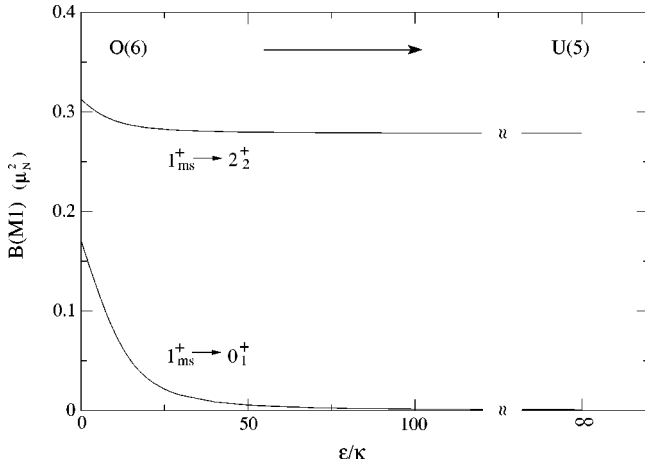


FIG. 6. The evolution of  $B(M1; 1_{ms}^+ \rightarrow 2_2^+)$  and  $B(M1; 1_{ms}^+ \rightarrow 0_1^+)$  absolute transition strengths as function of  $\epsilon/\kappa$  for a nucleus with  $N_\pi=1$  and  $N_\nu=5$ .  $0 \leq \epsilon/\kappa \leq \infty$  covers the transition between the dynamical O(6) and U(5) limits of the IBM-2.

choice of parameters predicts other properties of low-lying collective states in  $^{108}\text{Cd}$ . In Fig. 7, we compare the low-lying experimental excitation spectrum of  $^{108}\text{Cd}$  to calculations performed for  $\epsilon/\kappa=2$ , as well as for  $\epsilon/\kappa=14.46$ . The assumption  $\epsilon/\kappa=2$  reproduces the  $B(M1)$  ratio given in Eq. (5) but overpredicts the energy of the multiphonon  $0^+$  state. In fact, the calculated excited  $0^+$  state already belongs to the three-phonon multiplet, while in the experiment, this state lies between the two- and three-phonon multiplets. Obviously,  $\epsilon/\kappa=2$  is too close to the pure O(6) description.  $\epsilon/\kappa$

$=14.46$  reproduces the yrast band and the position of the excited  $0^+$  state nicely and underlines the transitional character of  $^{108}\text{Cd}$ ; but this choice of parameters predicts the  $B(M1)$  ratio (5) to be 5.53, inconsistent with the experimental observation for the  $1^+$  state at 3454 keV given above.

This paradoxical situation may be explained by quasiparticle admixtures. The level at 3454 keV decays to the intruder  $0^+$  as well as to the intruder  $2^+$  state implying quasiparticle contributions also in the wave function of this  $1^+$  state. In  $^{108}\text{Cd}$ , the characteristic proton intruder band based on the  $0_2^+$  state was established recently and is discussed in an earlier paper [10]. These admixtures are outside the model and may disturb the decay pattern predicted within the collective IBM-2. We stress that the absolute  $M1$  transition strengths of the  $1^+$  state at 3454 keV are too weak by at least a factor of 4, suggesting that the fragmentation of the  $1_{ms}^+$  state may be strong in  $^{108}\text{Cd}$ .

#### IV. ELECTRIC DIPOLE EXCITATIONS

Multiphonon excitations in even-even nuclei have been investigated extensively during the last decade (see Refs. [5,11], and references within). There is extensive knowledge about the coupling of isoscalar quadrupole phonons [32,33] which successfully serves to describe low-lying collective states with positive parity. The study of the coupling of various collective excitations is of great interest in nuclear structure physics. The crucial question is to what extent the fundamental building blocks of collective excitations can be combined. A particularly interesting problem is the coupling

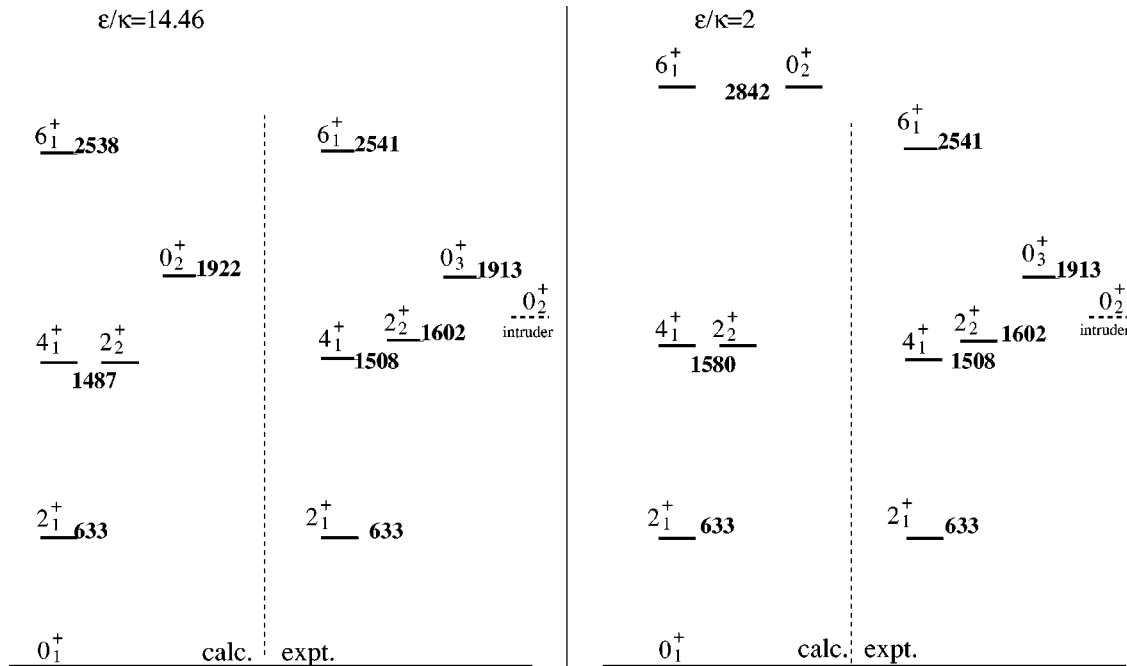


FIG. 7. Experimental low-lying spectrum in  $^{108}\text{Cd}$  compared to IBM-2 calculations ( $N_\pi=1$  and  $N_\nu=5$ ) using  $\epsilon/\kappa=14.46$  and  $\epsilon/\kappa=2$ . In the first case, the experimental energies are nicely reproduced and especially the position of the phonon  $0^+$  state is in good agreement. Please keep in mind that the  $0_2^+$  state observed in the experiment is the intruder band head and lies beyond the description of the IBM-2. The assumption  $\epsilon/\kappa=2$  chosen to reproduce the ratio  $B(M1; 1_{ms}^+ \rightarrow 2_2^+)/B(M1; 1_{ms}^+ \rightarrow 0_1^+)$  predicts the phonon  $0^+$  state to belong to the three-phonon multiplet at the energy of the  $6_1^+$  state.



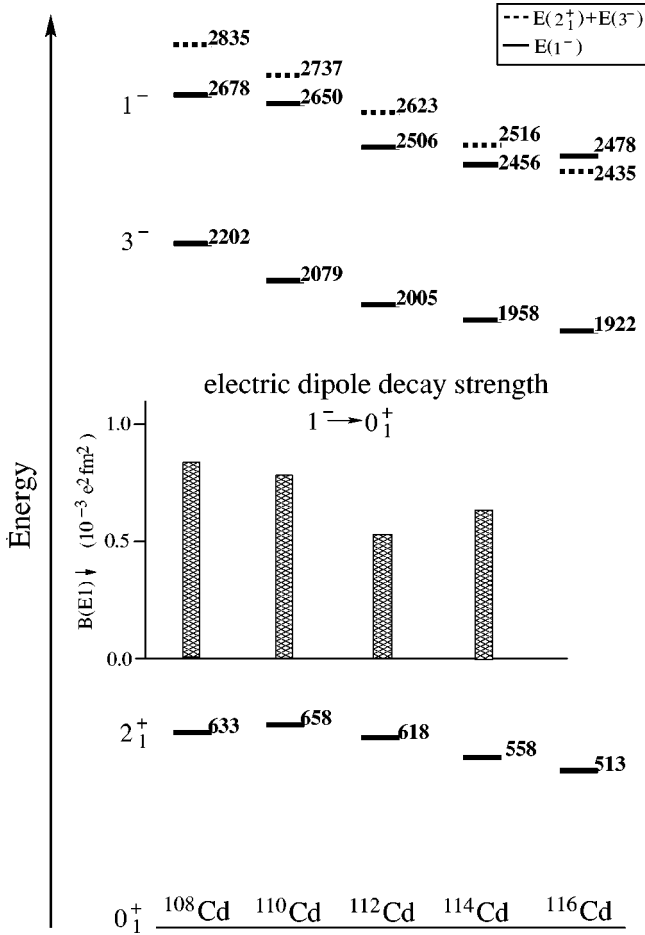


FIG. 8. Systematics of the  $(2_1^+ \otimes 3_1^-)$  coupled  $1^-$  states in  $^{108-116}\text{Cd}$ . The anharmonicity as well as the decay strength seem to increase towards the neutron deficient end, and the question arises if these tendencies are systematic. Further clarification can be obtained by an investigation of  $^{106}\text{Cd}$ . The data for  $^{110-116}\text{Cd}$  stem from Ref. [11].

of the lowest quadrupole and octupole modes resulting in the  $(2_1^+ \otimes 3_1^-)^{(J^-)}$ ,  $J=1,2,3,4,5$  quintuplet of states.

Experimental information is mostly confined to the  $1^-$  member of this quintuplet. The reason is that these states are easily accessible to the resonant photon scattering technique [6]. The heavier Cd isotopes with  $A=110-116$  have been subject of intensive NRF studies [11,12]. In a prior paper, we proposed the complete quadrupole-octupole coupled multiplet of negative parity in  $^{108}\text{Cd}$  based on excitation energies, decay properties, and a comparison to  $^{112}\text{Cd}$  [13]. Our aim of the present experiment was the determination of the absolute  $B(E1; 1^- \rightarrow 0_1^+)$  transition strength and the extension of the existing systematics on electric dipole excitations in the chain of even-mass Cd isotopes at its neutron deficient end. The suggested dipole member of the  $(2_1^+ \otimes 3_1^-)^{(J^-)}$  multiplet lies with 2678 keV about 5.5% below the sum energy of the  $2_1^+$  state (633 keV) and the first  $3^-$  level (2202 keV) [34].

In Table II, the decay properties of all states with negative and unknown parity are listed. For the three states with unclear parity assignment, we give absolute  $E1$ ,  $M1$ , and  $E2$

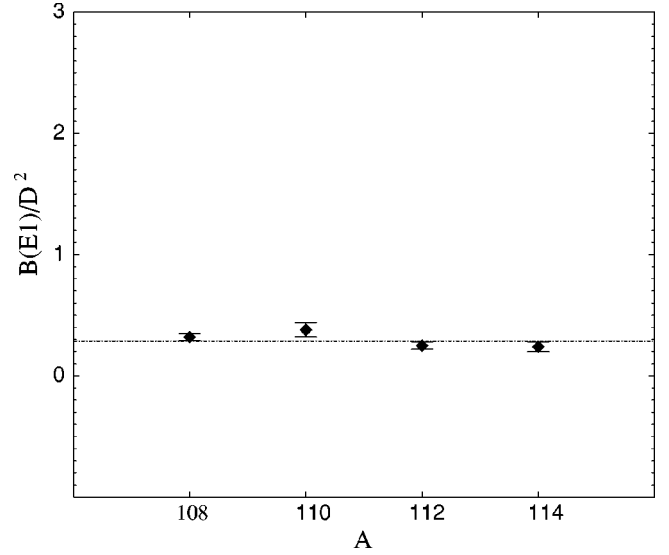


FIG. 9. Proportionality of the  $B(E1; 0^+ \rightarrow 1^-)$  excitation strength and the squared quadrupole and octupole deformation parameters within the chain of even-mass Cd isotopes.

transition strengths assuming pure multiplicities, respectively. In Fig. 8, we present the systematics of  $(2_1^+ \otimes 3_1^-)^{(J^-)}$  dipole excitations in  $^{108-116}\text{Cd}$  [11].  $^{108}\text{Cd}$  perfectly fits into the existing systematics of  $1^-$  states with increasing decay strength and an anharmonicity that seems to rise towards the neutron deficient end. However, the investigation of the neighboring  $^{106}\text{Cd}$  would clearly help to understand if these observations are solid tendencies and could contribute to the ongoing discussion on the evolution of anharmonicity for quadrupole-octupole coupled states [35].

To further prove the quadrupole-octupole two-phonon character of the  $1^-$  states discussed above, we investigate the empirically expected proportionality of the excitation strength and the product of the square of the quadrupole and octupole deformation parameters  $\beta_2$  and  $\beta_3$ :  $B(E1) \propto \beta_2^2 \beta_3^2$ . In Fig. 9,  $B(E1\uparrow)/D^2$  with  $D=5.376 \times 10^{-4} AZ \beta_2 \beta_3 e \text{ fm}$  [35–37] is given for the even-even  $^{108-114}\text{Cd}$  isotopes. The deformation parameters  $\beta_2$  and  $\beta_3$  are taken from Refs. [38,39] respectively, and the experimental  $B(E1)$  excitation strengths for  $^{110-114}\text{Cd}$  stem from Ref. [11]. The data points are scattered around the weighted mean of 0.29 and nicely underline the vibrational character as well as the two-phonon origin of these low-lying  $1^-$  states.

## V. CONCLUSION

Electric and magnetic dipole excitations in  $^{108}\text{Cd}$  were investigated in a nuclear resonance fluorescence measurement at the Stuttgart dynamitron accelerator using continuous bremsstrahlung with an end point energy of 4.1 MeV. We were able to determine lifetimes of eight dipole excitations for the first time. The  $1^+$  state at 3454 keV shows qualitatively a decay pattern meeting the expectations of the “scissors-mode-like”  $1_{ms}^+$  excitation in a nucleus located on a transitional path between vibrational U(5) and  $\gamma$ -soft O(6)

dynamical symmetry. The transitional character reflected by the decay properties of this  $1_{ms}^+$  candidate and the low-lying excitation spectrum were compared to IBM-2 calculations between the U(5) and O(6) dynamical limits. We found a contradictory situation, which may be explained by quasiparticle admixtures in the wave function of the  $1_{ms}^+$  candidate, affecting the decay pattern predicted within the purely collective IBM-2.

The lifetime of the quadrupole-octupole coupled  $1^-$  state at 2678 keV was determined for the first time in  $^{108}\text{Cd}$  and the deduced absolute  $E1$  decay strength as well as the excitation energy perfectly fits into the existing

systematics of the  $(2_1^+ \otimes 3_1^-)^{(1^-)}$  states in the chain of stable even-mass Cd isotopes.

#### ACKNOWLEDGMENTS

We thank Professor R. F. Casten, Professor A. Gelberg, Professor I. Wiedenhöver, Dr. N. Pietralla, Dr. S. Kasemann, Dr. A. Fitzler, and K. Jessen for valuable discussions. The authors from Köln thank the Institut für Strahlenphysik of the University Stuttgart for its kind hospitality during the NRF run. This work was partly supported by the Deutsche Forschungsgemeinschaft under Contract Nos. Br799/10–1 and Kn154/30.

- 
- [1] N. Lo Iudice and F. Palumbo, Phys. Rev. Lett. **41**, 1532 (1978); Nucl. Phys. **A326**, 193 (1979).
- [2] T. Otsuka, A. Arima, and F. Iachello, Nucl. Phys. **A309**, 1 (1978).
- [3] D. Bohle, A. Richter, W. Steffen, A.E.L. Dieperink, N. Lo Iudice, F. Palumbo, and O. Scholten, Phys. Lett. **137B**, 27 (1984).
- [4] A. Richter, Nucl. Phys. **A522**, 139c (1991), and references within.
- [5] C. Fransen, O. Beck, P. von Brentano, T. Eckert, R.-D. Herzberg, U. Kneissl, H. Maser, A. Nord, N. Pietralla, H.H. Pitz, and A. Zilges, Phys. Rev. C **57**, 129 (1998).
- [6] U. Kneissl, H.H. Pitz, and A. Zilges, Prog. Part. Nucl. Phys. **37**, 349 (1996).
- [7] J. Enders, N. Huxel, P. von Neumann-Cosel, and A. Richter, Phys. Rev. Lett. **79**, 2010 (1997).
- [8] J. Enders, H. Kaiser, P. von Neumann-Cosel, C. Ranga-charyulu, and A. Richter, Phys. Rev. C **59**, R1851 (1999).
- [9] A. Aprahamian, D.S. Brenner, R.F. Casten, R.L. Gill, and A. Piotrowski, Phys. Rev. Lett. **59**, 535 (1987).
- [10] A. Gade, J. Jolie, and P. von Brentano, Phys. Rev. C **65**, 041305(R) (2002).
- [11] W. Andrejtscheff, C. Kohstall, P. von Brentano, C. Fransen, U. Kneissl, N. Pietralla, and H.H. Pitz, Phys. Lett. B **506**, 239 (2001).
- [12] H. Lehmann, A. Nord, A.E. de Almeida Pinto, O. Beck, J. Besserer, P. von Brentano, S. Drissi, T. Eckert, R.-D. Herzberg, D. Jäger, J. Jolie, U. Kneissl, J. Margraf, H. Maser, N. Pietralla, and H.H. Pitz, Phys. Rev. C **60**, 024308 (1999).
- [13] A. Gade and P. von Brentano, Phys. Rev. C **66**, 014304 (2002).
- [14] N. Pietralla, I. Bauske, O. Beck, P. von Brentano, W. Geiger, R.-D. Herzberg, U. Kneissl, J. Margraf, H. Maser, H.H. Pitz, and A. Zilges, Phys. Rev. C **51**, 1021 (1995).
- [15] A. Gade, A. Fitzler, C. Fransen, J. Jolie, S. Kasemann, H. Klein, A. Linnemann, V. Werner, and P. von Brentano, Phys. Rev. C **66**, 034311 (2002).
- [16] P.E. Garrett, H. Lehmann, C.A. McGrath, Minfang Yeh, and S.W. Yates, Phys. Rev. C **54**, 2259 (1996).
- [17] N. Pietralla, C. Fransen, D. Belic, P. von Brentano, C. Friessner, U. Kneissl, A. Linnemann, A. Nord, H.H. Pitz, T. Otsuka, I. Schneider, V. Werner, and I. Wiedenhöver, Phys. Rev. Lett. **83**, 1303 (1999).
- [18] N. Pietralla, C.J. Barton III, R. Krücken, C.W. Beausang, M.A. Caprio, R.F. Casten, J.R. Cooper, A.A. Hecht, H. Newman, J.R. Novak, and N.V. Zamfir, Phys. Rev. C **64**, 031301(R) (2001).
- [19] H. Klein, A.F. Lisetskiy, N. Pietralla, C. Fransen, A. Gade, and P. von Brentano, Phys. Rev. C **65**, 044315 (2002).
- [20] G. Molnár, R.A. Gatenby, and S.W. Yates, Phys. Rev. C **37**, 898 (1988).
- [21] B. Fazekas, T. Belgya, G. Molnár, A. Veres, R.A. Gatenby, S.W. Yates, and T. Otsuka, Nucl. Phys. **A548**, 249 (1992).
- [22] I. Wiedenhöver, A. Gelberg, T. Otsuka, N. Pietralla, J. Gableske, A. Dewald, and P. von Brentano, Phys. Rev. C **56**, R2354 (1997).
- [23] N. Pietralla, D. Belic, P. von Brentano, C. Fransen, R.-D. Herzberg, U. Kneissl, H. Maser, P. Matschinsky, A. Nord, T. Otsuka, H.H. Pitz, V. Werner, and I. Wiedenhöver, Phys. Rev. C **58**, 796 (1998).
- [24] A. Gade, I. Wiedenhöver, J. Gableske, A. Gelberg, H. Meise, N. Pietralla, and P. von Brentano, Nucl. Phys. **A665**, 268 (2000).
- [25] W.D. Hamilton, A. Irbäck, and J.P. Elliott, Phys. Rev. Lett. **53**, 2469 (1984).
- [26] W.J. Vermeer, C.S. Lim, and R.H. Spear, Phys. Rev. C **38**, 2982 (1988).
- [27] J.R. Vanhoy, J.M. Anthony, B.M. Haas, B.H. Benedict, B.T. Meehan, S.F. Hicks, C.M. Davoren, and C.L. Lundstedt, Phys. Rev. C **52**, 2387 (1995).
- [28] J.N. Ginocchio, Phys. Lett. B **265**, 6 (1991).
- [29] F. Iachello and A. Arima, *The Interacting Boson Model* (Cambridge University Press, Cambridge, 1987).
- [30] P. van Isacker, K. Heyde, J. Jolie, and A. Sevrin, Ann. Phys. (N.Y.) **171**, 253 (1986).
- [31] T. Otsuka and N. Yoshida, JAERI-M 85-094 (Japan Atomic Energy Research Institute, Tokai-mara, Ibaraki, Japan, 1985).
- [32] G. Siems, U. Neuneyer, I. Wiedenhöver, S. Albers, M. Eschenauer, R. Wirowski, A. Gelberg, P. von Brentano, and T. Otsuka, Phys. Lett. B **320**, 1 (1994).
- [33] K. H. Kim, T. Otsuka, P. von Brentano, A. Gelberg P. van Isacker, and R. F. Casten, in *Capture  $\gamma$ -Ray Spectroscopy and Related Topics*, edited by G. Molnár (Springer, Budapest, 1996), Vol. 1, p. 195.

- [34] J. Blachot, Nucl. Data Sheets **81**, 599 (1997).
- [35] M. Babilon, T. Hartmann, P. Mohr, K. Vogt, S. Volz, and A. Zilges, Phys. Rev. C **65**, 037303 (2002).
- [36] A. Bohr and B.M. Mottelson, Nucl. Phys. **9**, 687 (1958).
- [37] F. Iachello, Phys. Lett. **160B**, 1 (1985).
- [38] S. Raman, C.H. Malarkey, W.T. Milner, C.W. Nestor, and P.H. Stelson, At. Data Nucl. Data Tables **36**, 1 (1987).
- [39] R.H. Spear, At. Data Nucl. Data Tables **80**, 35 (2002).